Forestry Studies | Metsanduslikud Uurimused, Vol. 79, Pages 3–20

Research paper

An experimental determination of the critical diffusion coefficient and critical relative humidity (RH) of drying air when optimizing the drying of three hardwood species (birch, aspen, and black alder)

Hannes Tamme*, Regino Kask, Peeter Muiste and Valdek Tamme

Tamme, H., Kask, R., Muiste, P., Tamme, V. 2023. An experimental determination of the critical diffusion coefficient and critical relative humidity (RH) of drying air when optimizing the drying of three hardwood species (birch, aspen, and black alder). – Forestry Studies | Metsanduslikud Uurimused 79, 3–20, ISSN 1406-9954. Journal homepage: http://mi.emu.ee/forestry.studies

Abstract. There are no systematic approaches available in current specialist literature when it comes to the optimization of the process of drying out hardwood species of wood, such as birch, aspen, or black alder, all of which find industrial uses in Estonia. In order to investigate the drying of these three hardwood species, this paper has made use of an experimental and theoretical drying optimization methodology which was developed previously for pine sapwood within the framework of the EIC Grant No. 16200 project. The same methodology was used to determine the critical diffusion coefficient and corresponding critical relative humidity levels (RH) in relation to the surrounding air, with those levels being important from the point of view of drying optimization, and calculating those levels separately for each species of hardwood. For alder it was found that the critical diffusion coefficient is Dcr = 36.57 * (10^{-4} mm^2 s^{-1}), while for aspen the figure was Dcr = 30.71 * (10^{-4} mm^2 s^{-1}), and for birch it was Dcr = 16.35 * (10^{-4} mm^2 s^{-1}). It was found that the time dependencies for the total deformation of different tree species tend to differ considerably, although the same drying regime was used for all of those tree species which were incorporated into the experiments.

Key words: wood drying, critical diffusion coefficient, effective diffusion coefficient.

Authors' address: Institute of Forestry and Engineering, Estonian University of Life Sciences, Kreutzwaldi 5, 51006 Tartu, Estonia; *e-mail: htamme@ut.ee

Introduction

There are no systematic approaches in currently available specialist literature regarding any optimization process for drying hardwood species (such as birch (*Betula* spp.), aspen (*Populus* spp.) or black alder (*Alnus glutinosa* (L.) Gaertn.)), at least those which have found any industrial use in Estonia. Various aspects of the industrial drying of spruce and pine wood, which are common in Estonia and the Nordic countries, have already been discussed most thoroughly, starting with purely practical tasks (Tronstad *et al.*, 2001; Poljakov, 2013; Mändoja, 2015; Naarits, 2018), and ending with the theory of drying (Salin, 1990, 2007).

DOI: 10.2478/fsmu-2023-0009

The pine and spruce wood drying simulation program TORKSIM (version 3.1 onwards), has significantly contributed towards the optimization of spruce and pine drying, both of these being common coniferous tree species in Estonia (Sova *et al.*, 2016; Tamme *et al.*, 2021b). With the help of the simulation, a drying schedule which lasts between one to two weeks can be resolved digitally in just a second or two (Tamme, 2023).

Mathematical models which are usually validated on the basis of experimental data which can be presented in the same article are less universal than TORKSIM. Sometimes such models contain important simplifying assumptions. For example, Baronas *et al.* (2002) assumed that the diffusion coefficient was constant with moisture content levels which were above FSP and which depended on a wood moisture content below FSP, according to the Arrhenius formula. In the work of Aboltins & Kic (2019), the high-temperature drying of biomass was studied and modelled with the help of small specimens which were made from five tree species (oak (*Quercus robur* L.), beech (*Fagus sylvatica* L.), spruce (*Picea abies* (L.) H. Karst.), Scots pine (*Pinus sylvestris* L.), and larch (*Larix decidua* Mill.)). The moisture contents of the wood being used in the experiments were close to absolute dry (0–3.5% for Scots pine and 0–6% (wet basis) for oak wood). In the paper (Danvind, 2005), the local diffusion coefficient was determined for spruce wood, based on Fick's first law and using the X-ray computed tomography method at different depths (2.0, 5.9, 9.8, 13.7, 17.6, 21.6, and 25.5 mm from the surface of the wood). In that research, it was found that the local diffusion coefficient values depended on the moisture content of the wood and the distance of the measuring volume of X-ray tomography from the surface of the wood to the centre of the wood. The moisture content of spruce wood in Danvind's experiments varied from 5% to 30% (dry basis), so the classic below-FSP moisture content region was used. In the paper by Tamme *et al.* (2021a), time dependences for wood moisture content from the beginning to the end of the drying period (0–120 hrs) were determined for pine sapwood at five different depths from the surface of the wood: 1 mm, 4 mm, 8 mm, 12 mm and 18 mm. The average moisture content of pine sapwood was varied in the laboratory experiment with a typical industrial drying plan, from the initial moisture level of 120% to the final moisture level of 26% (Tamme *et al.*, 2021a). Based on the experimentally discovered characteristic behaviour for the local diffusion coefficient of pine sapwood, the concept of the critical diffusion constant was defined for the surface layer of the wood (ca 2.5 mm deep from the surface). Regarding the discussion of this article, it was considered expedient to additionally determine the effective diffusion coefficients (EDC) for each tree species in a quasi-stationary drying regime using the methodology which had already been tested in previous papers (Tamme *et al.*, 2011; Tamme, 2016).

The main goal of this article was to apply the experimental and theoretical methodology which had been developed for the drying of pine sapwood, in order to now be able to determine the critical diffusion constant and corresponding critical drying air humidity for each hardwood species, something which is important in the optimization of hardwood drying.

Material and Methods

Theoretical background

The fundamental equation for the diffusion for non-stationary isothermal moisture transfer through the wood specimen represents Fick's second law in the one-dimensional case (Crank, 1956):

$$\frac{\partial u}{\partial t} = \frac{\partial}{\partial x}\left(D_t(T,u)\frac{\partial u}{\partial x}\right), \qquad (1)$$

where D_t is the diffusion coefficient perpendicular to the wood ($m^2 \cdot s^{-1}$).

When wood drying is carried out within a narrow temperature range of 50–60°C, that is, in a special isothermal case, then the simplified Fick's second law can be used:

$$D_{eff} \frac{\partial^2 u}{\partial x^2} = const, \tag{2}$$

where D_{eff} is the effective diffusion coefficient perpendicular to wood ($m^2 \cdot s^{-1}$).

The solution to such a differential equation is a polynomial of the second degree. A drying plan, one which considers the dynamics of moisture content and temperature, provides a parabolic distribution of the moisture content perpendicular to the surface of a material. This was referred to by Luikov as a quasi-stationary drying regime (Luikov, 1966; Tamme *et al.*, 2011).

The local diffusion coefficient can be experimentally determined according to Fick's first law (Fick, 1855; Crank, 1956; Salin, 1990; Tamme, 2016):

$$F = -D\frac{\partial u}{\partial x} \ , \tag{3}$$

where F is mass flux (kg/m^{2}s); D is the diffusion coefficient (m^2/s); u is mass concentration (kg/m^3); and x is the coordinate (m).

During the convective drying of wood, heat is transferred from the surrounding air through the surface of the wood into its interior and, at the expense of the heat energy being transferred to it, moisture evaporates from the wood, i.e. the wood is dried. The main equations are as follows when it comes to describing the heat flow of dry air, which is transferred to wood, and the heat flow of moist air which leaves the wood (Salin, 1990):

$$\O_1 = \alpha S(T_0 - T), \tag{4}$$

$$\O_2 = \beta c_p S(T_0 - T), \tag{5}$$

where $\O_1$ and $\O_2$ is the heat flow (W); α is the heat transfer coefficient (W/m^2 °C); ß is the mass transfer coefficient (m^2/s); c_p is the specific heat of humid air which is in equilibrium with the wood's surface (J/°C m^3); S is the surface area of the specimen (m^2); T_0 is the surrounding air temperature (°C); and T is the wood's surface temperature (°C).

The basic equation for the wood deformation calculation in the drying process is the following:

$$\frac{\partial \varepsilon}{\partial t} = \frac{1}{E}\frac{\partial \sigma}{\partial t} + \frac{\partial \varepsilon_v}{\partial t} + (\alpha + m\sigma)\frac{\partial \rho_b}{\partial t}, \tag{6}$$

where ε is total deformation; σ is tensile stress (Pa); E is the modulus of elasticity (Pa); ε_v is the viscoelastic strain; a is the unrestricted shrinkage coefficient (m^3 kg^{-1}); m is the mechano-sorptive creep coefficient (m^3 kg^{-1} Pa); ρ_b is the content of bound water (kg m^3); and t is time (s).

It should be kept in mind that the modulus of elasticity is not constant, but instead depends upon the wood moisture content and temperature (Salin, 1990).

Five out of eight measurement channels from the Scanntronik (Scanntronik, 2023) resistance meter were calibrated from a 10LogR resistance channel to the measurement channels for the wood moisture content (MC%), using a section-linear calibration model. In the section-linear calibration model (Tamme *et al.*, 2021a; Tamme, 2023), the following relationship holds true for each segment of the calibration function:

$$\frac{y - y_1}{y_2 - y_1} = \frac{x - x_1}{x_2 - x_1}, \tag{7}$$

where points A(x_1; y_1) and B(x_2; y_2) are the coordinates for the segment's endpoints.

The methodology for the individual calibration of the resistance-type wood moisture meter channels is described in more detail in Tamme's doctoral thesis (2023).

Formula (3) must be adapted to a suitable format in order to be able to process experimental data (i.e. MC%'s dependences on time *t* and coordinate *x*) in order to experimentally determine the local diffusion coefficient (Tamme *et al.*, 2021a). In principle, the diffusion coefficient (DC) can be given according to Formula (3) as the ratio of the mass flux to the gradient:

$$D = -\frac{Massflux}{Gradient}, \quad (8)$$

$$Massflux = -\Delta(MC\%)\frac{m_{dry}}{\Delta t * S}, \quad (9)$$

$$Gradient = \Delta(MC\%)\frac{\rho_{wood,dry}}{\Delta x}, \quad (10)$$

where D is the diffusion coefficient (DC) (m^2/s); while Δ(MC%) is the finite increment of the wood's MC% on the time axis for the mass flux and, in the material thickness (x-axis), for the gradient (MC%); m_{dry} is the wood dry mass (kg); S is the specimen surface area (m^2); Δt is the time increment (s); $\rho_{wood, dry}$ is the wood's dry density (kg/m^3); and Δx is the x coordinate's increment (m).

Materials

The drying experiments made use of three specimens of black alder, aspen, and birch which had been cut from the same materials, with a thickness of 35 mm, width of 150 mm, and length of 100 mm along the grain. The electrodes which are shown in the figure were placed on the first specimen. The second specimen in the drying experiments was intended for collecting drying curve data using the dry weight method. The third specimen was used for the individual calibration of electrodes by means of the slicing method (Tremblay *et al.*, 2000; Aboltins & Kic, 2019; Tamme *et al.*, 2021a; Tamme, 2023).

In all specimens listed here, moisture distribution was carefully obstructed in the longitudinal and tangential direction by means of special vapour barriers. Moisture could only leave the specimens in the radial direction. In this way a one-dimensional moisture gradient was guaranteed in the specimens (Tamme, 2023).

Experiment

Table 1. The same drying schedule for drying all hardwoods.

Time (h)	Surrounding air temp. (°C)	Wet bulb temp. (°C)	Surrounding air RH (%)
0	20	19.44	60
1	47	46.11	95
12	48	47.10	95
36	50	48.13	90
60	52	48.02	80
84	52	45.54	69
108	52	43.05	59
132	52	40.27	49

All of the experiments with the three hardwood species were carried out using the same drying plan (see Table 1). A FEUTRON climate chamber (Feutron, 2023) was used as a dryer. Only one tree species at a time was kept in the drying chamber. The drying time was 120 hours. A total of three drying sessions were conducted (one drying cycle for each hardwood species), following the plan shown in Table 1.

Sensors and collecting experimental data may be described as follows:

For a wood drying optimization system it is first necessary to develop reliable and accurate sensors to be able to record the average moisture, local moisture, and surface moisture levels in the wood, as well as a sensor to record the deformation of the wood surface. These sensors must simultaneously withstand temperatures of 50–80°C and high relative humidity levels of 95–100% RH which are characteristic of a convective kiln (Tamme *et al.*, 2021a).

The methodology for the experiment is described in more detail, together with photos, in the final report for the EIC contract No. 16200 (Tamme *et al.*, 2021b) and doctoral thesis (Tamme, 2023). The basic scheme for the experiment is shown in the photograph in Figure 1a and Figure 1b.

(a) (b)

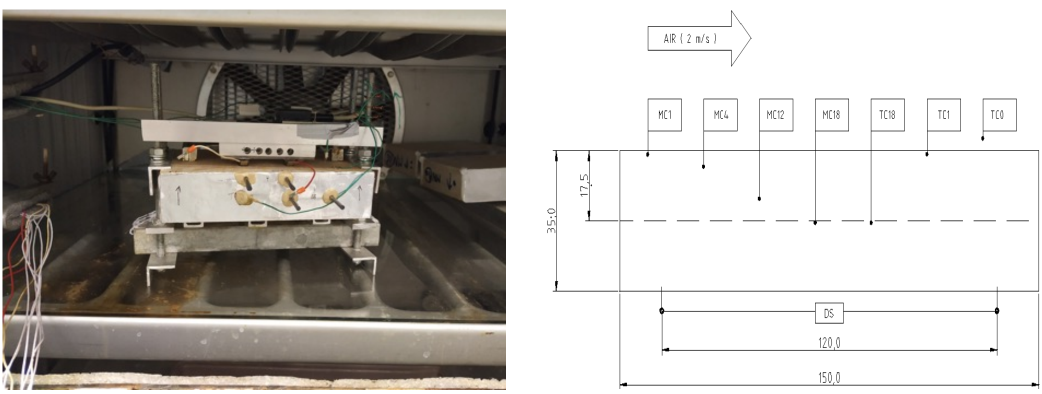

Figure 1. (a) interior view of the climate chamber, and (b) sensor placement schematic.

For the process of monitoring the drying process, the nine-channel data logger Almemo® 2890-9 was used, which is manufactured by Ahlborn (Ahlborn, 2023), as well as the eight-channel data loggers, Thermofox and Gigamodule, which are produced by Scanntronik (Scanntronik, 2023).

Statistical analysis

In the doctoral thesis (Tamme, 2023), the following hypothesis was established for pine sapwood:

'If the critical diffusion constant is exceeded, the drying process for the wood's surface layer will also affect the wood's inner layers.'

In the case of pine sapwood, the validity of this hypothesis was tested experimentally by means of a moistening pulse, along with calibrated and uncalibrated resistance sensors (Tamme *et al.*, 2021a).

To test the same hypothesis for hardwood species as part of this particular study, a statistical analysis was carried out in the freeware environment R (R Core Team, 2023) (see Table 5). The purpose of testing the hypothesis was to determine the strength of the linear relationship using the correlation coefficient, R, in layers with a depth of 1 mm and 12 mm. The 12 mm layer also served to characterise the average moisture content of the wood according to the EN 13183-2:2005 (2005) standard and the recommendations from EDG (Welling, 2010) (see Figure 2).

For data processing and figure formatting, use was made of the spreadsheet program Excel, and the freeware programs R (R Core Team, 2023) and MatPlotLib v3.4.3.

Results and Discussion

Table 2. Section-linear calibration functions determined on the basis of Formula (7) at depths of 1 mm and 4 mm from the surface, using the example of alder wood. Independent x-value is electrical resistance of wood (unit 10LogR). Dependent y-value is the moisture content (MC) of wood.

Depth (mm)	AB	BC	CD
1 mm	y = -8.0269x+475.3	y = -0.676x+61.97	y = -0.41x+43.335
4 mm	y = -12.813x+714.47	y = -1.474x+119.696	y = -0.721x+69.18

A total of 15 calibration functions at five different depths were determined for each hardwood species. A total of 45 calibration functions were determined for the three tree species.

For wood moisture content levels which were below FSP (< 30% MC), it was mathematically proven that the local moisture content of wood, as measured at a depth of a third of the material thickness from the surface, is numerically equal to the average wood moisture content level (Kretchetov, 1972). Even so, for wood moisture content levels which exceed FSP (> 30% MC), it is not clear whether the recommendation which is contained in the EN13183-2:2005 (2005) standard in regard to measuring the average moisture content at a depth of a third of the material thickness is in fact valid for every drying plan and every wood material thickness.

Figure 2 also presents an important result for the validation of the EN 13183-2:2005 (2005) standard for moisture content levels which exceed the FSP.

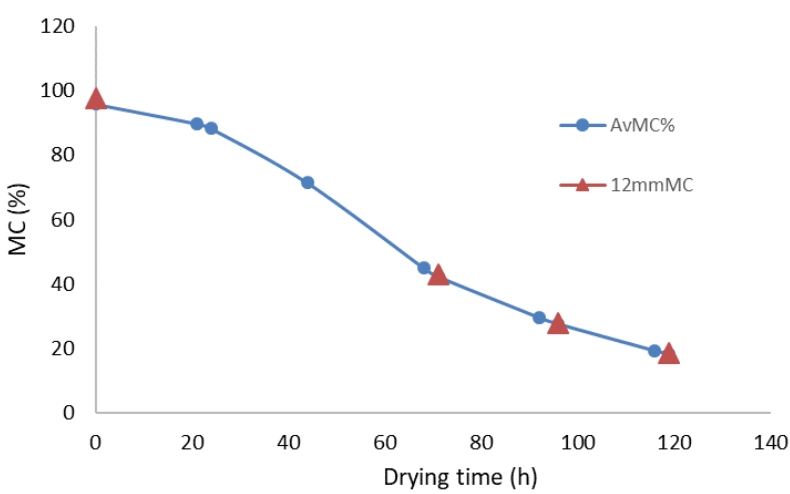

Figure 2. A comparison of the average moisture content levels, and the moisture content levels which were obtained using the slicing method at a depth of 12 mm on the example of alder wood.

Using alder wood as an example, the validation result confirms that the recommendation which is contained in the EN 13183-2:2005 (2005) standard to measure the average moisture content of wood at a depth of a third of the thickness is also relevant for moisture content levels which exceed the FSP, even without the corresponding mathematical proof.

The results from drying experiments using black alder wood

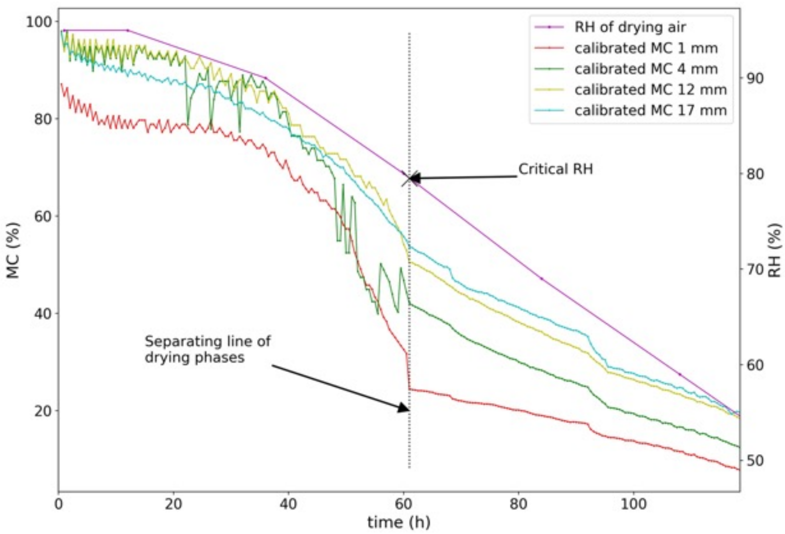

Figure 3. Alder wood drying experiment. Identification of the critical RH of the drying air according to the separating line of the first and second drying phase (Tamme *et al.*, 2021a). Drying curves for the layers of alder wood at different depths, and the RH graph for the drying air on an axis with a different scale, while the time axis is unchanged.

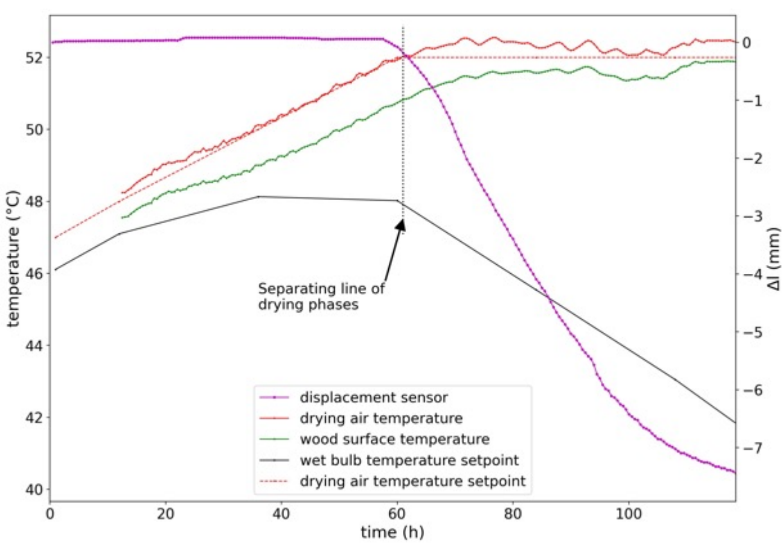

Figure 4. Alder wood drying experiment. Thermocouple data, with the temperature input based on the drying plan (see Table 1), and displacement sensor data depending on the drying time.

The results from drying experiments using aspen wood

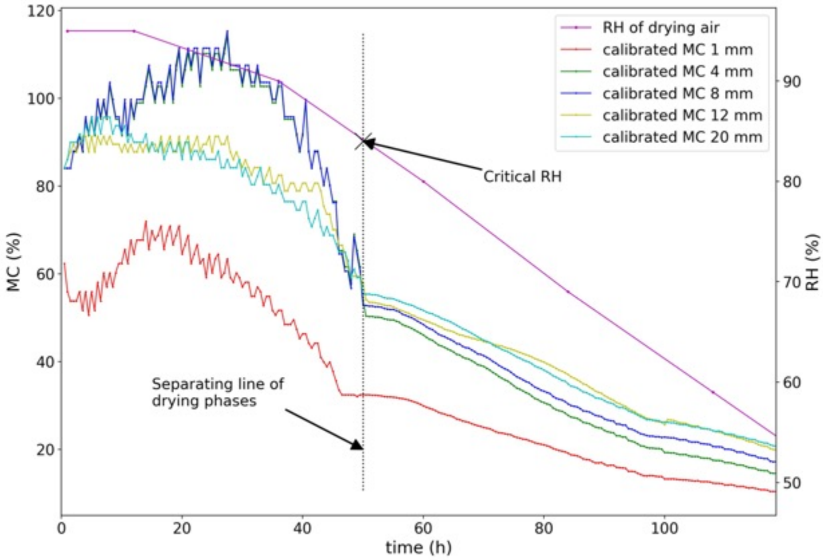

Figure 5. Aspen wood drying experiment. Identification of the critical RH of the drying air according to the separating line of the first and second drying phase. Drying curves for layers of aspen wood at different depths, and the RH graph for the drying air on an axis with a different scale, while the time axis is unchanged.

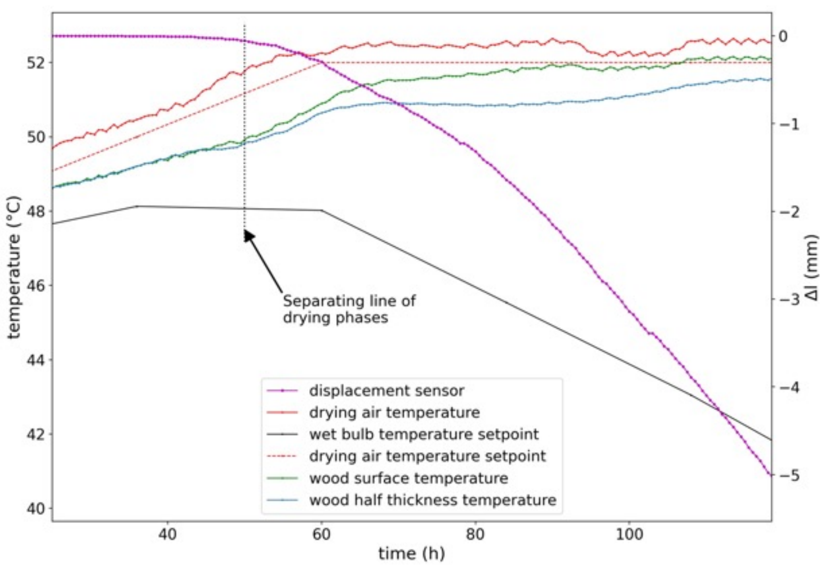

Figure 6. Aspen wood drying experiment. Thermocouple data, with temperature input based on the drying plan (see Table 1), and displacement sensor data depending on the drying time.

The results from birch wood-drying experiments

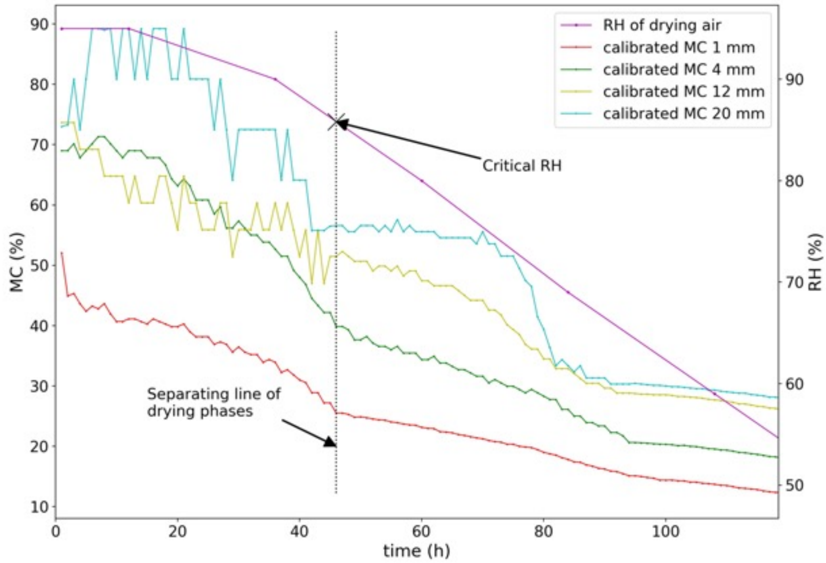

Figure 7. Birch wood drying experiment. Identification of the critical RH of the drying air according to the separating line of the first and second drying phase. Drying curves for layers of birch wood at different depths, and the RH graph for the drying air on an axis with a different scale, while the time axis is unchanged.

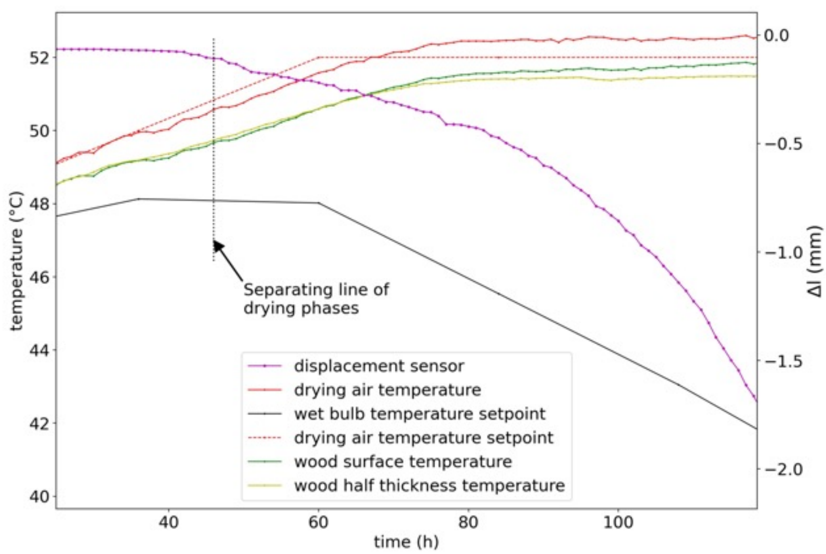

Figure 8. Birch wood drying experiment. Thermocouple data, with temperature input based on the drying plan (see Table 1), and displacement sensor data depending on the drying time.

A comparison of the results from drying experiments using different types of tree species

Table 3. The critical diffusion coefficient (Dcr) for the surface layer of three hardwood species and pine sapwood, along with the corresponding critical air humidity (RHcr) and the ratio of the diffusion coefficients for the first drying phase and the second drying phase in the surface layer (D_{cr}/D_{2ph}), for different tree species.

Type of wood	D_{cr} (*10^{-4} mm^2/s)	RH_{cr} (%)	D_{2ph} (*10^{-4} mm^2/s	D_{cr}/D_{2ph}
Black alder	36.57	75.6	13.87	2.64
Aspen	30.71	85.4	11.72	2.62
Birch	16.35	85.4	6.92	2.36
*Pine sapwood	27	81	18	1.5

Within the wood surface layer (in this study, about 2.5 mm from the wood surface), two local diffusion coefficients can be found, i.e. the local diffusion coefficient in the first drying phase for the surface layer, and the local diffusion coefficient in the second drying phase for the surface layer. The surface layer's local diffusion coefficient in which the wood's moisture content remains >FSP (i.e. greater than 30%) was referred to as the critical diffusion coefficient because, numerically speaking, it can be several times higher than the surface layer's diffusion coefficient in the second drying phase: "The maximum value of the diffusion coefficient immediately before entering into the second drying phase was named the *critical diffusion coefficient*." (Tamme *et al.*, 2021b; Tamme *et al.*, 2021a; Tamme, 2023).

Table 4. The experimentally determined moment of time, for the separating line (SL) and the corresponding average moisture content in the wood at the point at which the wood's surface layer transitions from the first drying phase into the second drying phase, and figures related to that transition.

Type of wood	Separating line (SL) (h) of drying phases	Avg MC (%)	Related figures
Black alder	61	55	Figure. 9, line 1; Figure. 11a
Aspen	50	62	Figure. 9, line 2; Figure. 11b
Birch	46	64	Figure. 9, line 3; Figure. 11c
*Pine sapwood	94	60	Figure. 11d

In Figure 9, line 1 is the transition for the alder wood surface layer from the first drying phase to the second drying phase; line 2 is the transition for the aspen wood surface layer from the first drying phase to the second drying phase; line 3 is the transition for the birch wood surface layer from the first drying phase to the second drying phase; and line 4 is the average wood moisture content which corresponds to the FSP value (i.e. 30% MC) for all of those tree species which were part of the experiment.

An additional explanation is required for Figure 9, line 4. If the wood average moisture content becomes lower than the FSP's corresponding average moisture content value (Figure 9, line 4), maximum drying stresses will begin to develop through-

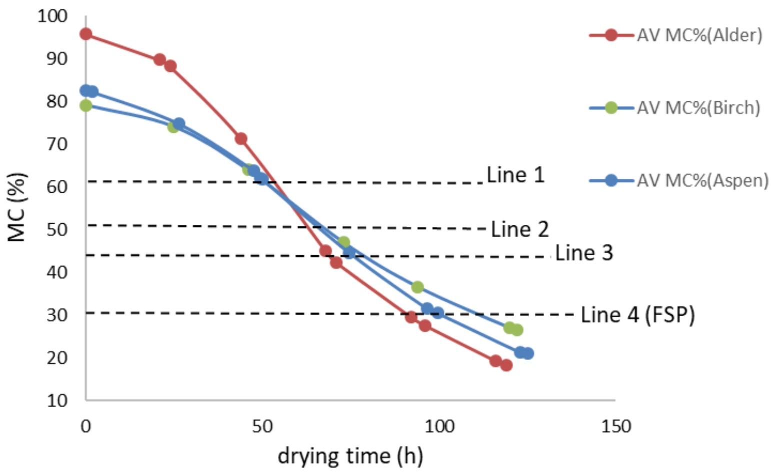

Figure 9.

A comparison of drying curves in different hardwood species under the same drying plan (see Table 1).

out the material at every depth. Therefore, if AvgMC < 30%, there is a risk of breaking stress developing in the material's surface layer (Salin, 1990; Tamme *et al.*, 2021b; Tamme, 2023). In the discussion section of Tamme's doctoral thesis, he explained that, although tensile stresses also occur in the surface layer only when the surface layer transitions to a situation in which the appropriate value falls beneath the FSP figure, apparently those stresses which are developed only in the surface layer are not numerically sufficient to create such a maximum tensile stress which would lead to the formation of drying cracks.

Testing the hypothesis for hardwood species

Table 5. Hypothesis testing results for hardwood species. Independent x-value is moisture content (MC) in the depth level of 1 mm from the surface. Dependent y-value is the MC in the depth level of 12 mm from the surface.

Type of wood	Equation: 12mmMC (y) ~ 1mmMC (x)	R	R^2	p-value
Black alder	y = 0.951x + 17.303	0.989	0.977	< 0.001
Aspen	y =1.275x + 11.8	0.979	0.958	< 0.001
Birch	y =1.302x + 12.028	0.965	0.931	< 0.001
*Pine sapwood	y =0.9377x + 57.898	0.992	0.984	< 0.001

According to Table 5 there is a strong linear relationship between the surface layer (1 mm) and the inner layer which corresponds to the average moisture content (12 mm) throughout the drying process, which itself indicates a causal relationship, i.e. the moisture content in the surface layer significantly affects the moisture content in the inner layers throughout the drying process. Consequently, the hypothesis which has already been established for pine wood (Tamme, 2023) is also valid for hardwoods.

Effective diffusion coefficient on a quasi-stationary state

Table 6. A comparison of the effective diffusion coefficient (EDC) (D_{eff}) for different tree species under quasi-stationary drying conditions.

Type of wood	D_{eff} ($*10^{-4}$ mm^2/s)
Black alder	11.92
Aspen	11.44
Birch	4.18
*Pine sapwood	9.58

An explanation is required for the definition of the effective diffusion coefficient (EDC). Formula (2) represents Fick's second law, in which the partial derivative with respect to time is assumed to be approximately constant, as it occurs in the quasi-stationary drying phase (Luikov, 1966; Salin, 1990; Tamme *et al.*, 2011). It is important to note that, according to Formula (2), the effective diffusion coefficient is the same at all depths from the wood surface, i.e. it no longer depends on the coordinate, as with the local diffusion coefficient which is determined based on Fick's first law (Formula (3)).

In Table 6, the given effective diffusion coefficient (EDC) was determined using the parabolas method (Kretchetov, 1972; Tamme *et al.*, 2011). The principle behind the parabolas method involves the parabolic moisture profiles (see Figures 10a–d and Table 7) containing all of the necessary information for determining the mass flux and gradient, and consequently also for determining the effective diffusion coefficient. According to Formula (2), in Fick's second law the mass flux becomes approximately constant, i.e. a quasi-stationary drying period occurs. In Figure 10a–d, the last two moisture profiles have almost parallel curves, which is a visual sign of the quasi-stationary state (Kretchetov, 1972; Tamme *et al.*, 2011).

Table 7. Equations of experimentally determined parabolic moisture profiles for different tree species, and an R-squared approximation. Independent x-value is the depth level (mm) from the board surface. Dependent y-value is the moisture content (MC%) at the depth level.

Type of wood	Time (h)	Equation of parabolic MC profile	R^2
Black alder	0	---------	------
(Figure 10a)	61	$y = -0.0976x^2 + 3.0933x + 30.2$	0.9512
	96	$y = -0.0655x^2 + 2.0568x + 12.884$	0.9964
	119	$y = -0.047x^2 + 1.5694x + 6.4665$	0.9974
Aspen	0	-----------	--------
(Figure 10b)	50	$y = -0.1197x^2 + 3.4894x + 32.592$	0.8463
	99.5	$y = -0.0597x^2 + 1.9168x + 11.8$	0.9916
	125	$y = -0.0315x^2 + 1.18x + 9.1838$	0.993
Birch	0	-----------	--------
(Figure 10c)	46	$y = -0.1154x^2 + 3.9316x + 23.5$	0.9698
	94	$y = -0.0599x^2 + 2.0472x + 13.274$	0.9981
	122	$y = -0.0547x^2 + 1.9479x + 10.274$	0.9984

Type of wood	Time (h)	Equation of parabolic MC profile	R^2
*Pine sapwood	22	$y = -0.054x^2 + 1.5471x + 91.484$	0.87
(Figure 10d)	92	$y = -0.0781x^2 + 2.3962x + 24.791$	0.8978
	116	$y = -0.0867x^2 + 2.2641x + 18.533$	0.8615
	140	$y = -0.0625x^2 + 1.8709x + 11.191$	0.9769

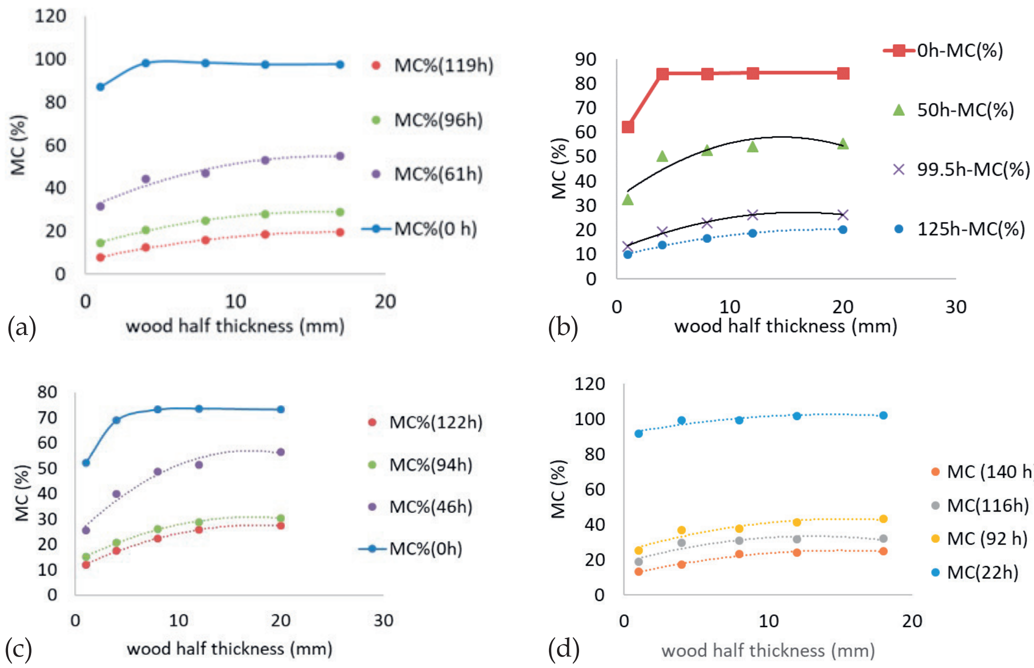

Figure 10. Moisture profiles for different tree species at different times of drying: (a) alder; (b) aspen; (c) birch; and (d) pine, with moisture profiles-based data which is used in the article (Tamme *et al.*, 2021a).

Maximum temperature differences between surrounding air and wood surface

For different tree species the characteristic maximum values were analysed for the difference between drying air and wood surface temperatures (see Figures 11a–d), which occur simultaneously in the material's critical surface layer (i.e. accelerated diffusion). Based on Formula (5), the heat flux of moist air which comes from the wood's surface is proportional to the temperature difference, with the comparison benchmarks being the mass transfer coefficient of moisture and the heat capacitance of the drying air. Therefore, it can be concluded that the maximum mass flux of moisture from the surface of the wood is also in sync with the critical diffusion coefficient in the surface layer of the wood, at approximately 2.5 mm deep from the surface. The physical reason for the temperature difference between the wood surface and the surrounding air is the fact that the thermal energy which is required for the evaporation of water (i.e. vaporisation heat or, approximately, enthalpy) is taken from the wood's surface, due to which the wood's surface is also cooled at the same time.

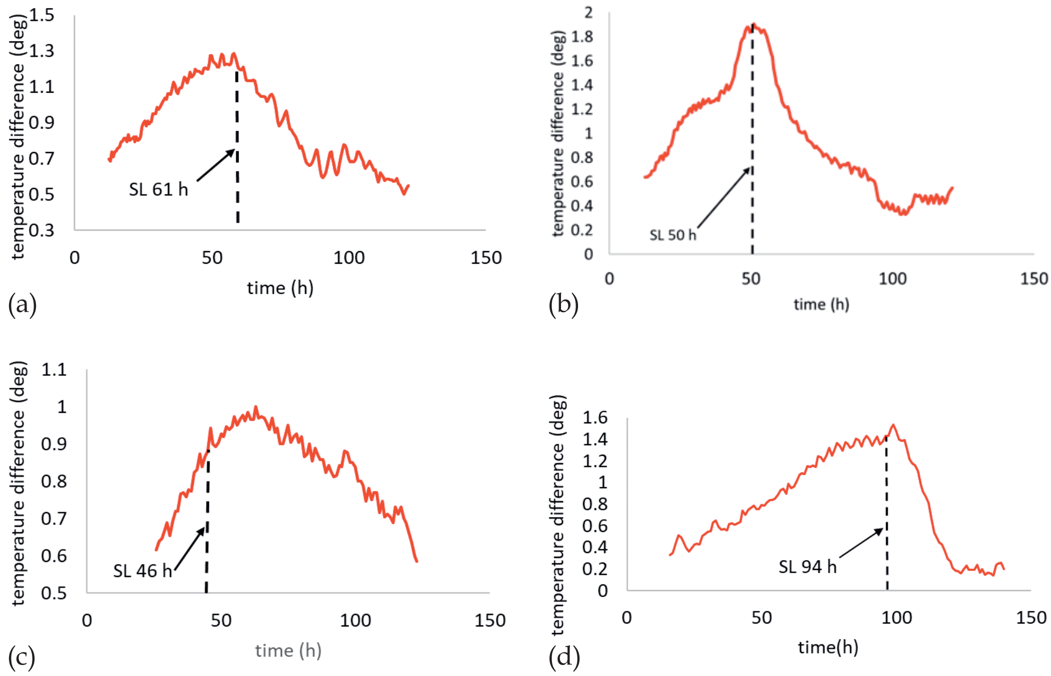

Figure 11. A comparison of differences in surrounding air temperature and wood surface temperature for different tree species: (a) alder; (b) aspen; (c) birch; and (d) pine (according to the paper by Tamme *et al.* (2021a)).

When comparing Figures 3, 5, 7 and Figure 11a–d, it can be concluded that the separating line (which is marked as 'SL' in the figures) for the first and the second drying phases within the surface layer is located in approximately the same position on the time axis as the specific maximum levels of the air and surface temperature difference (Figure 11a–d). Since the Dcr was determined on the basis of Figures 3, 5, 7, the maximum figures for temperature differences are therefore in sync with the Dcr figure which was achieved for all of the tree species. The maximum figures for temperature differences also form additional proof of the validity of the definition of the critical diffusion coefficient (Dcr) for the hardwood species.

The total deformation of the wood surface layer

The final stage of this process involves a look at the comparative behaviour of surface layer deformations (see Figure 13), which are calculated on the basis of Figure 12, and also on the basis of readings from the displacement sensor which monitored the shrinkage of the surface layer. A relevant analysis was carried out on different tree species and under the same drying plan conditions. The total experimental deformation of the surface layer was calculated by means of the following formula:

$$\text{Relative shrinkage} = \text{deformation} = (l_0 - l)/L \ (\text{mm/mm}), \qquad (11)$$

where l is the reading from the displacement sensor at time (t), while l_0 is the reading from the displacement sensor at the beginning of the surface layer's drying shrinkage process, and L is the length of the displacement sensor's base. In all tests, L=120 mm.

The total surface deformation as represented by the theoretical Formula 6 can

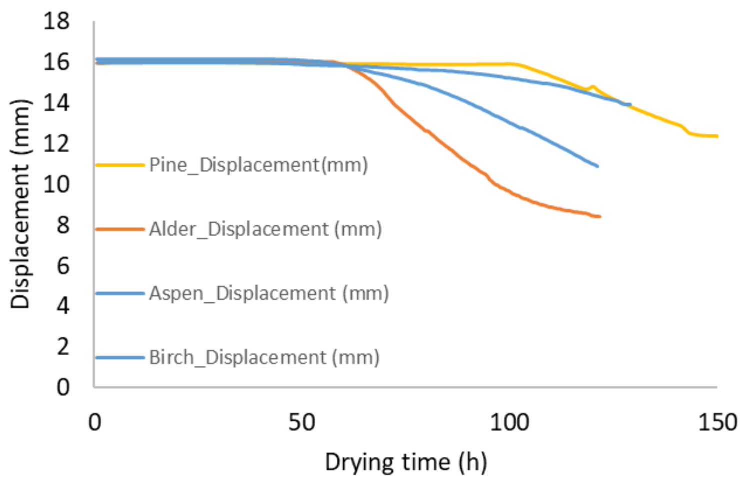

Figure 12.

A comparison of the behaviour of the surface layer displacement sensor as a function of time, for different tree species.

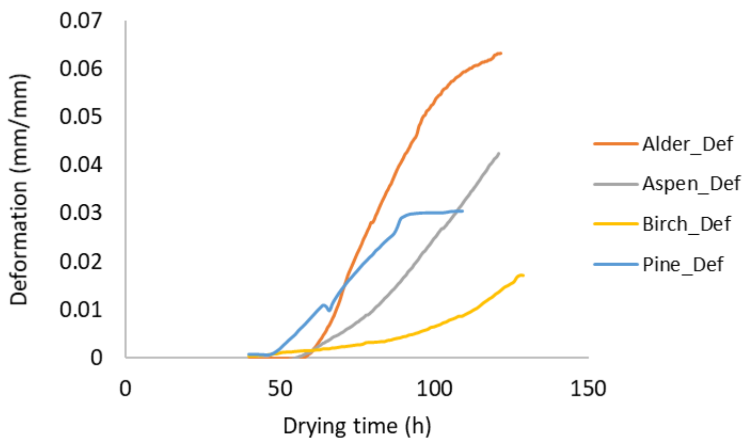

Figure 13.

A comparison of the total deformation in the surface layer depending on the drying time, for different tree species.

be considered as being a mathematical description of the wood's mechanical properties.

Formula 6 contains the components as additives when it comes to elastic deformation, viscoelastic deformation, and deformation which are all caused by mechanosorption (Salin, 1990). Figure 13 shows that the total deformation according to the aforementioned formula is linearly dependent upon time for pine sapwood and alder. In the case of birch and aspen, the dependence of the total deformation on time is rather exponential, which suggests that the wood modulus of elasticity (MOE) is not linearly dependent upon the wood moisture content. Another possibility is that the MOE retains a linear dependence upon the wood's moisture content, but the viscoelastic deformation dominates, which is indeed basically an exponent function (Salin, 1990).

Conclusions

The experimental and theoretical drying methodology which has been developed for pine sapwood under the EIC Grant No. 16200 project also worked surprisingly well in terms of the study of hardwood drying. The methodology clearly highlighted quite important differences between the process of drying hardwoods and that of drying pine sapwood. At the same time, the basic definitions were confirmed for the methodology, sometimes in an even more prominent form when compared to that for pine wood (see Table 3). For all species of hardwood which were used in the tests, the existence of a critical diffusion coefficient was confirmed in the surface layer, as well as the maximum values for the difference between the drying air temperature and that of the wood's surface which is something that occurs practically in sync with the Dcr. The effective diffusion coefficients found at the beginning of the quasi-stationary drying period were also highly comparable (see Table 6). When comparing the total deformations in the surface layer of pine wood and hardwoods (see Figure 13), the influence of the mechanical properties of different wood species was vividly highlighted in terms of the dynamics behind the total deformation. And, finally, with the help of statistical analysis, the basic hypothesis which had been set up for pine sapwood in the doctoral thesis (Tamme, 2023) in regard to the transfer of changes in the wood's surface layer to its inner layers (see Table 5) was proved also to be true for hardwood species.

Acknowledgments. This work was supported by the Environmental Investment Centre of Estonia (Grant No. T220055MIMP (RE.4.08.22-0049)).

References

Aboltins, A., Kic, P. 2019. Determination of the mass diffusion coefficient of wood by thin-layer drying kinetics. – Agronomy Research, 17(1), 5–12.

Ahlborn. [WWW document]. – URL http://www.ahlborn.com. [Accessed 22 October 2023].

Baronas, R., Ivanauskas, F., Sapagovas, M. 2002. Reliability of one dimensional model of moisture diffusion in wood. – Informatica, 13(4), 405–416.

Crank, J. 1956. The Mathematics of Diffusion. Oxford, Clarendon Press. 347 pp.

Danvind, J. 2005. Analysis of drying wood based on nondestructive measurements and numerical tools. – Doctoral thesis. Luleå, Sweden, Luleå University of Technology. 124 pp.

EN 13183-2:2005. 2005. Moisture content of a piece of sawn timber – Part 2: Estimation by electrical resistance method. Brussels, Belgium, European Committee for Standardization 6 pp.

Feutron Klimasimulation GmbH. [WWW document]. – URL https://www.feutron.de/en/weathering-chamber/. [Accessed 22 October 2023].

Fick, A. 1855. Ueber Diffusion. – Pogendorff, J.C. (ed.). Annalen der Physik und Chemie, Vol. 94, 59–86. (In German).

Kretchetov, I.V. 1972. Kiln Drying. (Сушка древесины). Moscow, Lesnaya Promyshlennost. 440 pp. (In Russian).

Luikov, A.V. 1966. Heat and Mass Transfer in Capillary-Porous Bodies. New York, Pergamon Press. 523 pp.

Mändoja, M. 2015. Wood drying simulation "TORKSIM" adjusting to actual industrial drying curve in order to improve the reliability of tension calculations and electrical humidity sensors. ((Puidu kuivatuse simulatsiooniprogrammi "TORKSIM" sobitamine reaalse tööstusliku kuivatuskõveraga, eesmärgiga tõsta pinge arvutuste ja elektriliste niiskusandurite usaldusväärsust). – Bachelor thesis. Tartu, Estonian University of Life Sciences. 51 pp. (In Estonian with English summary).

Naarits, A. 2018. Optimization of drying quality and energy consumption of Scots pine and Norway spruce lumber in AS Aegviidu Puit – a case study. (Männi- ja kuusepuidu kuivatuse kvaliteedi ja energiakulu optimeerimise võimalused AS Aegviidu Puit kuivatite näitel). – Master thesis. Tartu, Estonian University of Life Sciences. 77 pp. (In Estonian with English summary).

Poljakov, A. 2013. Wood material comparison of actual moisture content monitoring data in wood dryer "Mühlböck" and "Hekotek". (Puitmaterjali tegeliku niiskussisalduse võrdlus monitooringu andmetega puidu kuivatites "Mühlböck" ja "Hekotek"). – Master thesis. Tartu, Estonian University of Life Sciences. 125 pp. (In Estonian).

R Core Team. 2023. R: A language and environment for statistical computing. R Foundation for Statistical Computing, Vienna, Austria. [WWW document]. – URL http://www.r-project.org/. [Accessed 13 April 2023].

Salin, J.G. 1990. Simulation of the timber drying process. Prediction of moisture and quality changes. – Doctoral thesis. Helsinki, Finland, EKONO Oy. 103 pp.

Salin, J.G. 2007. Lectures. Riga, 2007. [WWW document]. – URL http://www.coste53.net/downloads/WG2/WG2-Riga/Lectures/Riga2007-Salin.pdf. [Accessed 22 October 2023].

Scanntronik Mugrauer GmbH. [WWW document]. – URL www.scanntronik.de/. [Accessed 22 October 2023].

Sova, D., Bedelean, B., Sandu, V. 2016. Application of Response Surface Methodology to optimization of wood drying conditions in a pilot-scale kiln. – Baltic Forestry, 22(2), 348–356.

Tamme, H. 2023. Development of control and optimization methods for wood drying. – Doctoral thesis. Tartu, Estonian University of Life Sciences. 181 pp.

Tamme, H., Muiste, P., Tamme, V. 2021a. Optimizing the pine wood drying process using a critical diffusion coefficient and a timed moistening impulse. – Forestry Studies / Metsanduslikud Uurimused, 75, 150−165.

Tamme, V. 2016. Development of resistance-type control methods for wood drying. – PhD thesis. Tartu, Estonian University of Life Sciences. 135 pp.

Tamme, V., Muiste, P., Mitt, R., Tamme, H. 2011. Determination of effective diffusion coefficient and mechanical stress of pine wood during convective drying. – Baltic Forestry, 17(1), 110–117.

Tamme, V., Tamme, H., Muiste, P. 2021b. Development of experimental and theoretical methodology for optimization of quality and energy consumption of convective drying of wood (chamber drying and tunnel drying. (Puidu konvektiivkuivatuse (kamberkuivatus ja tunnelkuivatus) kvaliteedi ja energiakulu optimeerimise eksperimentaalse ja teoreetilise metoodika välja töötamine.) – KIK metsanduse programmi projekti nr. 16200 lõpparuanne, 44 pp. [WWW document]. – URL https://mi.emu.ee/userfiles/instituudid/mi/MI/Projektid/Projekt1620.pdf. [Accessed 22 October 2023]. (In Estonian).

Tremblay, C., Cloutier, A., Fortin, Y. 2000. Experimental determination of the convective heat and mass transfer coefficients for wood drying. – Wood Science and Technology, 34(3), 253–276. https://doi.org/10.1007/s002260000045.

Tronstad, S., Sandland, K.M., Toverød, H. 2001. Drying quality of softwood based on 140 industrial tests in Norwegian sawmills and actions to improve the quality. – Proceedings of the 3 rd workshop of COST Action E15 on softwood drying to specific end-uses. Advances in the drying of wood (1999-2003). Finland, 11-13 June, Helsinki, 13 pp.

Welling, J. 2010. Dried timber - how to specify correctly. European Drying Group (EDG) and COST E53. 38 pp.

Kolme lehtpuu liigi (kask, haab, lepp) kuivatuse optimeerimise jaoks kriitilise difusiooni teguri ja kriitilise kuivatusõhu suhtelise niiskuse (RH) eksperimentaalne määramine

Hannes Tamme, Regino Kask, Peeter Muiste ja Valdek Tamme

Kokkuvõte

Eestis tööstuslikku kasutust leidvate lehtpuude (sanglepp, haab, kask) kuivatuse optimeerimise kohta puuduvad erialakirjanduses süstemaatilised käsitlused. Selles artiklis kasutati kolme lehtpuu liigi kuivatuse uurimisel varem männi maltspuidu jaoks Keskkonnainvesteeringute Keskuse (KIK) projekti nr 16200 raames välja töötatud eksperimentaalset ja teoreetilist kuivatuse optimeerimise metoodikat. Sama metoodika alusel määrati iga lehtpuu liigi jaoks eraldi kuivatuse optimeerimise seisukohalt olulised kriitilised difusiooni koefitsiendid ja vastavad kriitilised kuivatusõhu suhtelised niiskused (RH). Lepapuidu jaoks leiti, et kriitiline difusiooni koefitsient on Dcr = 36,57 * (10^{-4} mm^2 s^{-1}), haavapuidul Dcr = 30,71 * (10^{-4} mm^2 s^{-1}) ja kasepuidul Dcr = 16,35 * (10^{-4} mm^2 s^{-1}). Katseliselt saadud puidu niiskusprofiilide (st niiskussisalduse 1D jaotused sõltuvana kaugusest puidu pinnast) alusel määrati paraboolide meetodiga lisaks efektiivsed difusiooni koefitsiendid kvaasistatsionaarse kuivatusrežiimi alguses: lepa puhul Deff = 11,92 * (10^{-4} mm^2 s^{-1}), haab Deff = 11,44 * (10^{-4} mm^2 s^{-1}), kask Deff = 4,18 * (10^{-4} mm^2 s^{-1}) ja võrdlusena männi maltspuidu jaoks leiti Deff = 9,58 * (10^{-4} mm^2 s^{-1}). Lõpuks määrati ja võrreldi erinevate puuliikide pinnakihi kogudeformatsiooni väärtusi sõltuvana kuivatuse ajast. Leiti, et erinevate puuliikide kogudeformatsiooni sõltuvused ajast erinevad omavahel tunduvalt, kuigi kasutati sama kuivatusrežiimi kõigi katsetes osalenud puuliikide korral.

Männi maltspuidu jaoks KIK-i projekti nr 16200 raames välja töötatud kuivatuse eksperimentaalne ja teoreetiline metoodika töötas üllatavalt hästi ka lehtpuude kuivatuse uurimisel. Metoodika tõi hästi välja lehtpuude küllaltki olulised erinevused, võrreldes männi maltspuidu kuivatamisega. Samal ajal leidsid kinnitust metoodikapõhilised definitsioonid mõnikord veelgi reljeefsemal kujul, võrreldes männipuiduga (vt tabel 3). Kõigi katsetes kasutatud lehtpuu liikide kohta leidsid kinnitust pinnakihi kriitilise difusiooni koefitsiendi olemasolu, ja Dcr-iga praktiliselt sünkroonis esinevad kuivatusõhu ja puidu pinnatemperatuuride vahe maksimumid. Edukalt sai omavahel võrrelda ka leitud efektiivsed difusiooni koefitsiendid kvaasistatsionaarse kuivatusperioodi alguses (vt tabel 6). Männipuidu ja lehtpuude pinnakihi kogudeformatsioonide võrdlemine (vt joonis 13) tõi ilmekalt esile erinevate puuliikide mehaaniliste omaduste mõju kogudeformatsiooni dünaamikale. Lõpuks tõendati statistilise analüüsi abil selles artiklis lehtpuude korral doktoritöös (Tamme, 2023) männi maltspuidu jaoks püstitatud põhiline hüpotees puidu pinnakihis toimuvate muutuste üle kandumise kohta puidu sisekihtidesse (vt tabel 5).

Lehtpuude kuivatusplaane võib soovi korral samuti TORKSIM-i abil simuleerida, kuid siis tuleks simulatsiooni tulemusi alati võrrelda lehtpuude vastavate katseandmetega (kõigepealt kuivamiskõveraid omavahel ja ka niiskusprofiile valitud võrdluspunktides, temperatuure jne). Lehtpuude kuivatuse praktiliste probleemide lahendamiseks võiks panustada uudse spetsiifilise anduri, st kuivamispingete maksimumi indikaatori (Tamme *et al.*, 2021a) arendamisse.